PHYSICAL REVIEW A **73**, 020703(R) (2006)

Laser-driven target of high-density nuclear-polarized hydrogen gas

B. Clasie,[1] C. Crawford,[1] J. Seely,[1] W. Xu,[2] D. Dutta,[2] and H. Gao[1,2]
[1]*Laboratory for Nuclear Science, Massachusetts Institute of Technology, Cambridge, Massachusetts 02139, USA*
[2]*Triangle Universities Nuclear Laboratory, Duke University, Durham, North Carolina 27708, USA*
(Received 12 October 2005; published 16 February 2006)

We report the best figure-of-merit achieved for an internal nuclear polarized hydrogen gas target and a Monte Carlo simulation of spin-exchange optical pumping. The dimensions of the apparatus were optimized using the simulation, and the experimental results were in good agreement with the simulation. The best result achieved for this target was 50.5% polarization with 58.2% degree of dissociation of the sample beam exiting the storage cell at a hydrogen flow rate of 1.1×10^{18} atoms/s.

DOI: 10.1103/PhysRevA.73.020703 PACS number(s): 34.50.Ez, 29.25.Pj, 32.80.Bx

The exploitation of polarization observables through the use of polarized beams and polarized internal gas targets in storage rings is an increasingly valuable technique in nuclear and particle physics. Nucleon properties, such as the spin structure functions and the electromagnetic form factors, have been measured in recent years with polarization techniques utilizing polarized internal targets at DESY (HERMES), NIKHEF, and the MIT-Bates Laboratory. The spin-dependent asymmetry from the $\vec{p}+\vec{p}\rightarrow p+p+\phi$ process has been suggested [1,2] as a possible probe of the strangeness content of the nucleon. The near-threshold $\vec{p}+\vec{p}\rightarrow Y+\Theta^+$ process could be used to determine the parity of the Θ^+ pentaquark state [3–5], if its existence is confirmed.

The laser-driven target (LDT) is capable of producing nuclear polarized hydrogen and deuterium for storage rings. The LDT and the atomic beam source (ABS) (another technique more commonly used) both use storage cells [6] to increase the target thickness, compared to a free gas jet target. However, the LDT offers a more compact design than the ABS, and can provide a higher figure of merit (FOM) [30] as reported in this work. An LDT was first used in nuclear physics experiments [7,8] in 1997 and 1998 at the Indiana University Cyclotron Facility following earlier work on the laser-driven source and target [9–12]. A hydrogen LDT project was initiated at MIT in the late 1990s with the goal of implementing such a target in the South Hall Ring at the MIT-Bates Linear Accelerator Center for a precision measurement of the proton charge radius [13,14]. In this paper, we report the best FOM result obtained from this target, which benefited from the development of a realistic Monte Carlo (MC) simulation of the target.

An LDT is based on the technique of spin-exchange optical pumping. The valence electron of potassium is polarized through optical pumping in a magnetic field of ~1 kG using circularly polarized laser light. Spin-exchange collisions then transfer the polarization from potassium to the hydrogen (H) electron. Finally, the hyperfine interaction during H-H collisions transfers the electron spin to the nucleus [15,16]. If there are many H-H collisions, the rate of transfer of spin to the nucleus equals the reverse rate, and the system is in spin temperature equilibrium (STE) [17]. The time constant for STE is approximately given by [17]

$$\tau_{\mathrm{STE}}=\frac{1+(B/B_c)^2}{n_{\mathrm{H}}\sigma_{\mathrm{SE}}^{\mathrm{HH}}v_{\mathrm{rel}}^{\mathrm{HH}}}, \tag{1}$$

where B_c is the critical magnetic field (507 G for hydrogen), n_{H} is the density of atomic hydrogen (excluding molecular hydrogen), $\sigma_{\mathrm{SE}}^{\mathrm{HH}}$ is the thermally averaged H-H spin exchange cross section at the temperature of the spin-exchange cell, and $v_{\mathrm{rel}}^{\mathrm{HH}}$ is the average relative velocity between hydrogen atoms. Laser-driven sources and targets are designed with the dwell time constant in the spin-exchange cell much greater than the STE time constant to guarantee that the system is in STE. Moreover, STE has been verified in laser-driven sources and targets [18–20]. Under STE conditions, the hydrogen nuclear and electron polarizations are equal [18].

The main contributions to depolarization of the alkali-metal and hydrogen in our apparatus come from the flow of atoms into and out of the LDS and depolarization during wall collisions [21]. Atoms may also recombine at a surface producing molecules with predominantly zero net nuclear spin. The recombination is characterized by the degree of dissociation, f_α, which is the fraction of the hydrogen flux in the sample beam exiting the storage cell that is in atomic form. Drifilm coatings are employed to limit the recombination and depolarization effects from wall collisions [22]. The depolarization from radiation trapping [23,24] can be limited by optical pumping in a large magnetic field in the kG range [17]; however, the rate of transfer of spin to the nucleus by the hyperfine interaction is reduced. Therefore, the magnitude of the magnetic field in the spin-exchange cell must be optimized for these two competing effects [17,21,25].

Figure 1 is a schematic view of the MIT LDT. Hydrogen gas flows successively into different sections of a piece of pyrex glassware (which consists of a dissociator tube, a spin-exchange cell, and a transport tube) and an aluminum storage cell. The molecular gas is dissociated into atoms by an rf discharge in the dissociator tube. In the spin-exchange cell, the hydrogen gas (now a mixture of atoms and molecules) is mixed with the potassium vapor produced in a side-arm by heating a potassium ampoule. The results from two spin-exchange cells, "Original" and "Large-1," are reported herein. To minimize the number of wall collisions, the Original spin-exchange cell design was spherical with an inner

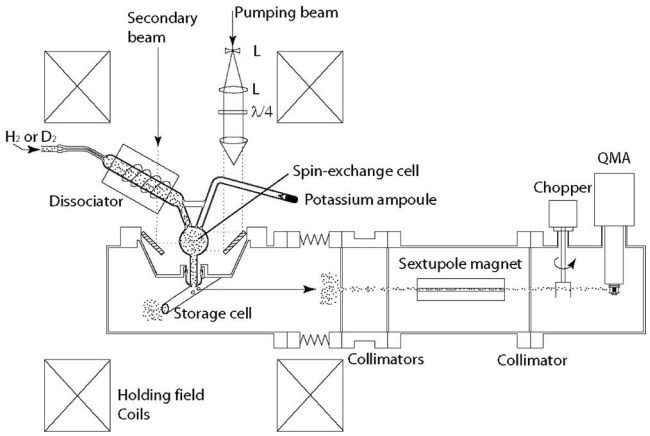

FIG. 1. Laser-driven target setup. Note that, for clarity, the polarimeter arm, storage cell, dissociator, and potassium ampoule are shown rotated by 90° from their actual positions (in the actual setup, the polarimeter arm and ampoule would come out of the page). An optional secondary beam can be used to measure the alkali-metal density and polarization via a Faraday polarimeter.

diameter of 4.8 cm. Large-1 was a cylindrical cell optimized by the MC simulation described below. The entire volume contained by the spin-exchange cell, transport tube, and storage cell must be heated to 200–250 °C to prevent the alkali-metal vapor from condensing on the walls, which would degrade the drifilm coating. The potassium number density is typically 0.3% compared to H. The standard storage cell is an open-ended aluminum cylinder coated with drifilm. The cell is 40 cm in length and 1.25 cm in diameter with two sampling holes allowing the target gas to be monitored by an atomic polarimeter. One hole is centered and the other one is 15 mm downstream. Both are positioned at right angles to the entrance hole of the storage cell, which ensures that the atoms monitored by the atomic polarimeter undergo wall collisions in the storage cell before escaping the cell. A MC simulation determined that atoms that exit the center (off-center) sampling hole experience, on average, 1370 (1370) wall collisions of which 135 (155) wall collisions are in the storage cell.

The laser used is a titanium-sapphire laser (Ti:sapphire) pumped with a 20 W argon ion laser. The laser beam passes through an electro-optic modulator (EOM, not shown), an expanding lens, and a quarter-wave plate before arriving at the spin-exchange cell via a periscope with two polarization-preserving mirrors. The EOM broadens the relatively narrow linewidth of the Ti:sapphire laser to provide a better match to the potassium Doppler absorption profile with a FWHM of 1.0 GHz. In addition, two sampling beams are split off from the pump beam for monitoring the laser spectrum and wavelength.

Gas exiting the sampling hole of the storage cell is collimated through a series of apertures which also serve as conductance limiters between subchambers of the polarimeter. A permanent sextupole magnet focuses one electronic spin state of the atomic beam and defocuses the other. The optimal focal length was determined by an atomic beam simulation. The beam is then sampled by a quadrupole mass analyzer (QMA) which alternately measures both the atomic and molecular intensities. The QMA is shielded from the holding field by two layers of μ-metal. The small signal at $\sim$1 m from the storage cell is enhanced using a chopper along with a lock-in amplifier. The background pressure is reduced to 10^{-9} Torr by differentially pumping the two subchambers with ion pumps and also a NEG pump in the second (QMA) chamber. The background can be measured by blocking the beam with a shutter or rotating the polarimeter away from the sampling hole.

TABLE I. FOM results from the HERMES ABS [26–28], IUCF LDT [20], and the MIT LDT. The units are as follows; the flow, F (10^{16} atoms/s); the thickness, t (10^{13} atoms/cm^2); the FOM, $F\langle p_z\rangle^2$ (10^{16} atoms/s); and, the FOM, $t\langle p_z\rangle^2$ (10^{13} atoms/cm^2). All LDT results for f_α are under operating conditions, with the potassium ampoule heated.

	HERMES (ABS)		IUCF (LDT)		MIT LDT	
					Original	Large-1
Gas	H	D	H	D	H	H
F	6.57	5.15	100	72	110	110
t	11	[10.5]	50	50	150	150
f_α			$\sim$0.48	$\sim$0.48	0.56	0.58
P_e			$\sim$0.45	$\sim$0.45	0.37	0.50
$\langle p_z\rangle$	0.78	0.85	0.145	0.102	[0.175]	[0.247]
$F\langle p_z\rangle^2$	4.0	3.8	2.1	0.75	3.4	6.7
$t\langle p_z\rangle^2$	6.7	7.6	1.1	0.52	4.6	9.2

The degree of dissociation of the sample beam exiting the storage cell is given by the change in the molecular signal (after subtracting the background) when the rf discharge is turned on and off. The electron polarization of the atomic hydrogen species, P_e, is given by the change in the atomic signal when the laser is turned on and off by opening or closing a laser shutter (after subtracting the background). This measurement also indicates the hydrogen nuclear polarization, as the system is designed to be in STE. The mean dwell time for atomic hydrogen in the Original spin-exchange cell and transport tube has been calculated by a MC simulation to be 8.8 ms. For a field of 100 mT and an atomic hydrogen density of 1.0×10^{14} atoms/cm^3, the time constant for STE given by Eq. (1) is 0.052 ms. The mean dwell time is therefore larger than the STE time constant by a factor of approximately 170. The Erlangen hydrogen LDS was verified to be in STE by directly measuring the nuclear polarization [18] in conditions where the mean dwell time was larger than the STE time constant by a factor of 300, and the system was expected to remain in STE at half that ratio.

Results from the IUCF and MIT LDTs are summarized in Table I along with results from the HERMES ABS. The FOM is given as (flow)$\times\langle p_z\rangle^2$ and (thickness)$\times\langle p_z\rangle^2$, where $\langle p_z\rangle$ is the density averaged nuclear vector polarization. For the MIT LDT,

$$\langle p_z\rangle = \frac{f_\alpha P_e}{f_\alpha + \sqrt{2}(1-f_\alpha)}. \tag{2}$$

For the IUCF target, $\langle p_z\rangle$, was determined from a scattering experiment [7,20]. The results for the flow and target thick-

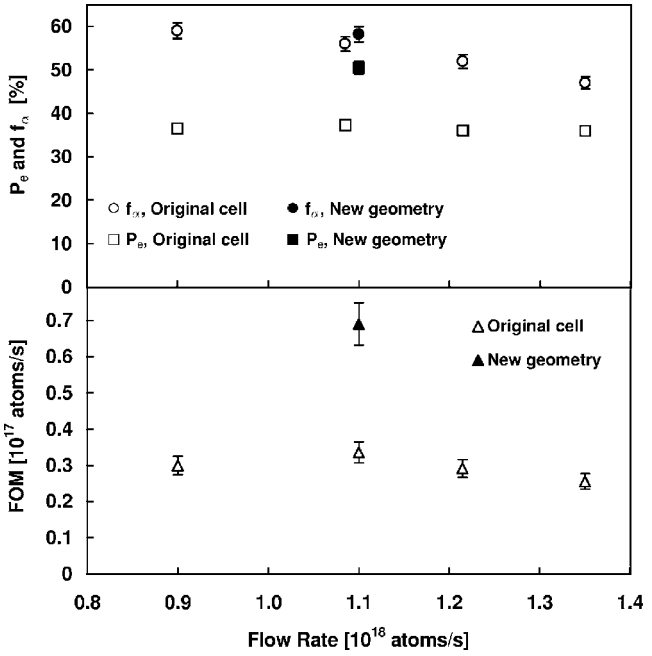

FIG. 2. Results achieved by the MIT LDT. The FOM is given as $(\text{flow}) \times \langle p_z \rangle^2$, where $\langle p_z \rangle$ is the density averaged H nuclear vector polarization assuming the system is in STE.

ness of the HERMES ABS are based on Refs. [26–28], and are the best published ABS results that use a storage cell.

The best results achieved by the MIT LDT in the Original configuration are shown in Fig. 2 together with the overall errors, which are dominated by the systematic errors. The combined systematic uncertainty in the FOM is estimated to be 8.4%, which is dominated by the nonlinearity in the QMA response (less than 3%), hydrogen flow control (4%), and 3% in the density averaged target polarization. The measurements were repeated several times for this cell geometry under various conditions, including recoating the surface, with reproducible results.

A detailed MC simulation of optical pumping and spin-exchange collisions for our target was developed and used to extract the recombination and depolarization coefficients, and to provide a new cell design to improve the target performance. The simulation techniques developed for the LDT are also applicable to the design of the ABS, particularly at future facilities where constraints may cause significant recombination and/or spin exchange. The recombination coefficient, $\gamma_r(n_\mathrm{H})$, is the probability for a hydrogen atom to recombine at a wall collision and is a function of n_H near the surface. As n_H varies throughout the simulated volume, γ_r changes with position on the surfaces.

In the simulation, a hydrogen atom moves ballistically between wall collisions in the spin-exchange cell, transport tube, and storage cell. A new velocity, both magnitude and direction, is randomly generated after each wall collision, according to a Maxwellian and a $\cos\Theta$ distribution, respectively, where Θ is the polar angle measured with respect to the normal to the surface. At high temperatures, which are experienced in an LDT, the recombination coefficient, γ_r, is given by [29]

$$\gamma_r(n_\mathrm{H}) = C_\mathrm{H} n_\mathrm{H}, \tag{3}$$

where C_H is a constant. After the hydrogen atom exited either through a sampling hole or the ends of the storage cell, another hydrogen atom was generated at the top of the spin-exchange cell.

The MC was used to determine n_H throughout the apparatus. As n_H depends on the average probability that atoms have not recombined at a given point, and this probability depends on n_H through Eq. (3), the simulation was iterated and n_H recalculated after each iteration until the degree of dissociation of atoms exiting the storage cell sampling hole and n_H converged.

Although the hydrogen atoms were transported separately, H-H and H-K spin-exchange collisions were treated by allowing the hydrogen atoms to interact with the average hydrogen electron and nuclear polarization and potassium electron polarization. The apparatus was divided into a three-dimensional $2 \times 2 \times 2$ mm^3 grid. Initial values of the average H and K polarizations were assigned at every point on the grid. After a hydrogen atom exited the apparatus in the simulation, the average polarizations were updated, and the simulation was iterated until convergence. A hydrogen atom can be depolarized during a wall collision with the probability given by the depolarization coefficient, γ_p. The MC results were fit to the experimental results for the Original configuration, shown in Table I, by varying C_H and γ_p, which were determined to be 3.33×10^{-18} cm^3 and 0.00355, respectively. Further discussion of the MC simulation will be reported in a forthcoming paper.

A cylindrical spin-exchange cell with a much larger diameter was constructed based on the MC studies and the practical constraints of our target chamber. The calculated mean dwell time divided by the STE time constant was 280. This design, labeled Large-1 in Table I, has a spin-exchange cell volume 6.8 times larger than that of the Original design. The best result obtained for this cell using the EOM was $P_e = 50.5\%$ and $f_\alpha = 58.2\%$ at a flow rate of 1.1×10^{18} atoms/s. These results are in good agreement with the MC simulation, which predicted $P_e = 57\%$ and $f_\alpha = 51\%$ at the same flow rate.

While in the Original configuration, drifilm coatings were found to last in excess of 100 h under operating conditions, the polarization result for the Large-1 cell was stable at 50% polarization for about 12 h but with rather rapid deterioration of the dissociation fraction. This observation may have been due to uneven heating of the spin-exchange cell and the transport tube. For the Large-1 geometry, there was only a 1 cm gap for the hot air to circulate around the glass due to the constraint of the existing target chamber. One can overcome this constraint with the design of a new target chamber.

One may argue that it is probably not completely justified to compare the performance of the HERMES ABS target and the IUCF LDT with the FOM of the LDT obtained in our polarized target lab due to the difference in the storage cell conductances. A detailed study shows that minimal modifications are needed for the installation of this target in the MIT-Bates storage ring. A more realistic comparison, which takes into account correction factors due to the target geometry, temperature, and molecules, still shows that our target

with the Large-1 cell geometry has a $(33\pm11)\%$ higher figure of merit than that of the HERMES hydrogen target. These results represent an even larger improvement compared to the previous best FOM from an LDT, which was obtained at IUCF. A similar comparison that does not bias toward the MIT LDT due to the storage cell conductance is $(210\pm30)\%$ higher than the IUCF result. These comparisons will be explained in a forthcoming paper.

We thank Tom Wise and Willy Haeberli for the construction of the storage cells; Michael Grossman and George Sechen for their technical support; Ernest Ihloff, Manouchehr Farkhondeh, William Nispel, and Defa Wang for their help with the vacuum chamber, the laser system, fabrication of the spin-exchange cell oven, and the rf system; Tom Hession for the fabrication of the spin-exchange cells; and T. Black for his help in the early stage of this project. We appreciate the useful discussions with Hauke Kolster. We thank J. Stewart and P. Lenisa for the information on the HERMES ABS target. This work is supported in part by the U.S. Department of Energy under Contract No. DE-FC02-94ER40818. H.G. acknowledges the support from the DOE.

[1] A. I. Titov, B. Kampfer, and B. L. Reznik, Eur. Phys. J. A **7**, 543 (2000).
[2] A. I. Titov, B. Kampfer, and V. V. Shklyar, e-print nucl-th/9811094.
[3] A. W. Thomas, K. Hicks, and A. Hosaka, Prog. Theor. Phys. **111**, 291 (2004).
[4] C. Hanhart, J. Haidenbauer, K. Nakayama, and U.-G. Meissner, Phys. Lett. B **606**, 67 (2005).
[5] Yu. N. Uzikov, e-print nucl-th/0411113.
[6] E. Steffens and W. Haeberli, Rep. Prog. Phys. **66**, 1887 (2003).
[7] R. V. Cadman *et al.*, Phys. Rev. Lett. **86**, 967 (2001).
[8] M. A. Miller *et al.*, in *Proceedings of the International Workshop on Polarized Gas Targets and Polarized Beams, Urbana, 1997* (American Institute of Physics, New York, 1998), p. 148.
[9] R. J. Holt *et al.*, in *Proceedings of the Eighth International Symposium on High-Energy Spin Physics, Minneapolis, 1988* (American Institute of Physics, New York, 1989), p. 1535.
[10] M. Poelker *et al.*, Phys. Rev. A **50**, 2450 (1994).
[11] H. Gao *et al.*, in *Proceedings of the International Workshop on Polarized Beams and Polarized Gas Targets, Cologne, 1995* (World Scientific, Singapore, 1996), p. 67.
[12] J. Stenger, M. Beckmann, C. Grosshauser, N. Koch, W. Nagengast, and K. Rith, in *Proceedings of the International Workshop on Polarized Beams and Polarized Gas Targets, Cologne, 1995* (World Scientific, Singapore, 1997), p. 85.
[13] H. Gao, Int. J. Mod. Phys. E **12**, 1 (2003).
[14] H. Gao and J. R. Calarco, Proposal to MIT-Bates PAC 00-02 (2000).
[15] W. Happer, Rev. Mod. Phys. **44**, 169 (1972).
[16] J. Wilbert, Ph.D. thesis, University of Erlangen (2002).
[17] T. Walker and L. W. Anderson, Nucl. Instrum. Methods Phys. Res. A **334**, 313 (1993).
[18] J. Stenger, C. Grosshauser, W. Kilian, B. Ranzenberger, and K. Rith, Phys. Rev. Lett. **78**, 4177 (1997).
[19] J. A. Fedchak, K. Bailey, W. J. Cummings, H. Gao, R. J. Holt, C. E. Jones, R. S. Kowalczyk, T. O'Neill, and M. Poelker, Nucl. Instrum. Methods Phys. Res. A **417**, 182 (1998).
[20] R. V. Cadman, Ph.D. thesis, University of Illinois at Urbana-Champaign (2001).
[21] J. Stenger and K. Rith, Nucl. Instrum. Methods Phys. Res. A **361**, 60 (1995).
[22] J. A. Fedchak *et al.*, Nucl. Instrum. Methods Phys. Res. A **391**, 405 (1997).
[23] D. Tupa and L. W. Anderson, Phys. Rev. A **36**, 2142 (1987).
[24] D. Tupa, L. W. Anderson, D. L. Huber, and J. E. Lawler, Phys. Rev. A **33**, 1045 (1986).
[25] L. W. Anderson and T. Walker, Nucl. Instrum. Methods Phys. Res. A **357**, 220 (1995).
[26] A. Airapetian *et al.*, Nucl. Instrum. Methods Phys. Res. A **540**, 68 (2005).
[27] M. Capiluppi, Absolute determination of the target density for the transverse H running (2002-2005), HERMES internal note (2005).
[28] M. Henoch, HERMES internal report 02-029 (2002).
[29] H. Kolster, Ph.D. thesis, Ludwig-Maximilians-Universität München (1998).
[30] The FOM is a measure of the performance of a polarized target, which determines the statistical uncertainty of an asymmetry measurement for a given beam time.